

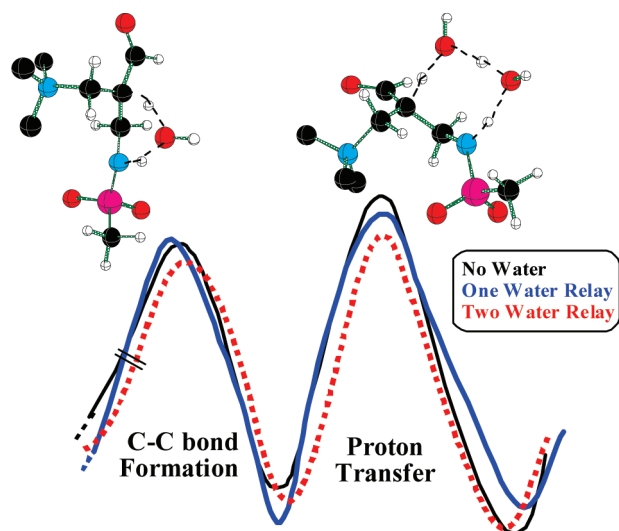
## Mechanistic Insights and the Role of Cocatalysts in Aza-Morita–Baylis–Hillman and Morita–Baylis–Hillman Reactions

Dipankar Roy, Chandan Patel, and Raghavan B. Sunoj\*

Department of Chemistry, Indian Institute of Technology Bombay, Mumbai 400076, India

*sunoj@chem.iitb.ac.in*

Received March 24, 2009



The mechanism of the trimethylamine or trimethylphosphine catalyzed aza-Morita–Baylis–Hillman (MBH) reaction between acrolein and mesyl imine is investigated by using ab initio and density functional methods. All key transition states are located at the CBS-4M as well as at the mPW1K/6-31 + G\*\* levels of theories. To account for the experimentally known rate enhancements through the use of polar protic cocatalysts, transition state models with explicit cocatalysts are considered. Inclusion of polar protic cocatalysts is found to have a profound influence in decreasing the activation barriers associated with the key elementary steps. The protic cocatalysts such as water, methanol, and formic acid are identified as effective in promoting a relay proton transfer. Interestingly, the efficiency of the relay mechanism results in relatively better stabilization of the proton transfer transition state as compared to the addition of enolate to the electrophile (C–C bond formation). The cocatalyst bound models suggest that the proton transfer could become the rate-determining step in the aza-MBH reaction under polar protic conditions. A comparison of the aza-MBH reaction with the analogous MBH reaction is also attempted to bring out the subtle differences between these two reactions. Enhanced kinetic advantages arising from the nature of the activated electrophile are noticed for the aza-MBH reaction. The difference in the relative energies between the transition states for the proton transfer and the C–C bond formation steps with bound cocatalyst(s) is found to be more pronounced in the aza-MBH reaction. In general, the reported results underscore the importance of considering explicit solvents/cocatalysts in order to account for the likely role of the specific interactions between reactants and solvents/cocatalysts.

### Introduction

The Morita–Baylis–Hillman (MBH) reaction has been recognized as one of the effective strategies toward

generating highly functionalized compounds through C–C bond formation.<sup>1</sup> The most common versions of the MBH reaction involve the reaction of an activated olefin with an aldehyde in the presence of a nucleophilic Lewis base catalyst, more often a tertiary amine or a phosphine. Over the

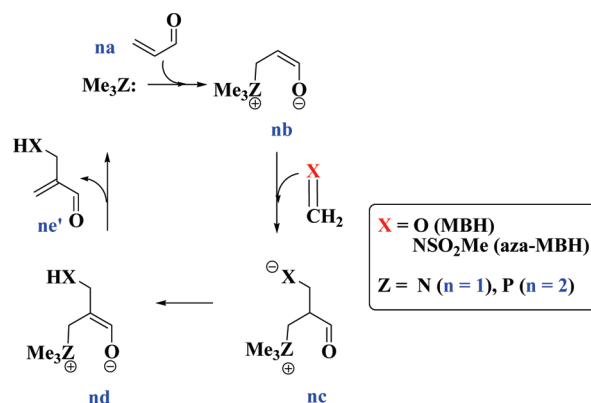
\*To whom correspondence should be addressed. Fax: (+91) 22-2576-7152.

years, the reactions has been demonstrated as capable of encompassing a broad range of substrates, wherein a tandem Michael-aldol sequence is proposed to be involved.<sup>2</sup> Since its introduction the MBH reaction has indeed played a vital role in achieving complex molecular targets.<sup>3</sup> The MBH adducts have also been subjected to further synthetic manipulations into a variety of compounds such as azetidines,<sup>4</sup>  $\beta$ -amino acids,<sup>5</sup> and epoxides.<sup>6,7</sup>

Among the range of electrophiles employed in the MBH reaction, the use of activated imine received special attention. In what is commonly known as the aza-Morita–Baylis–Hillman reaction, an activated imine is reacted with standard Michael acceptors as in the MBH reaction.<sup>8</sup> For instance, the improved electrophilicity imparted by sulfonated imino groups in aza-MBH reaction and tunability by varying the nature of imino substituents render wider scope for furthering the applications of the MBH reaction.<sup>9,10</sup> More importantly, the aza-MBH reaction has also been demonstrated as a viable route toward realizing asymmetric MBH products.<sup>11</sup>

Akin to the MBH reaction, the mechanistic investigations on aza-MBH are not widely available in the literature. The substrate similarity between these two reactions has naturally prompted many to propose a common mechanism. The general reaction sequence, in the absence of any protic species, can be envisaged to include (i) Michael addition of the Lewis base to an activated olefin, (ii)

### SCHEME 1. The General Mechanism Proposed for the MBH Reaction



zwitterionic intermediate thus generated to an aldehyde or imine acceptor, (iii) intramolecular proton transfer, and (iv) expulsion of the Lewis base to furnish the MBH product (Scheme 1). Such a mechanistic scheme for the MBH reaction under polar aprotic conditions was earlier reported from our laboratory.<sup>12</sup> A closer perusal of the available experimental reports conveys that either the addition of the enolate to the electrophile (b–c) or an intramolecular proton transfer (c–d) is regarded as the rate-limiting step in the aza-MBH reaction.<sup>9d,e</sup> The relative magnitudes of the activation barriers for these steps are not convincingly established by using sound experimental studies as yet.

It is to be reckoned that the widespread applications of MBH reaction are known to suffer from twin limitations of slow reaction rates and poor conversions. While there are several methods reported toward improving the speed of the MBH reaction, the use of polar protic additives or cocatalysts appears to be a reasonably well-accepted protocol.<sup>13</sup> In this context, it is important to note that the rate-determining step (RDS) in the MBH reaction has long been proposed to be the C–C bond formation step.<sup>14</sup> In a few studies, the key intermediates involved in the MBH reaction have been isolated and characterized.<sup>15</sup> This scenario, however, could change drastically in the presence of polar protic additives in the reaction medium.<sup>9d,16</sup> The nature of the RDS is not yet unequivocally established under these conditions. A number of qualitative propositions are available on the likely role of polar protic species on the mechanistic course of the MBH reaction. These studies generally emphasize the hydrogen bonding stabilization of polar transition states or a more direct participation by the polar protic species (vide infra). In a related study, the role of the hydrophobic effect toward improving the rate of the MBH reaction is postulated to be of

(1) (a) Baylis, A. B.; Hillman, M. E. D. German Patent 2155113, 1972; *Chem. Abstr.* **1972**, 77, 34174q. (b) Morita, K. Japan Patent 6803364, 1968; *Chem. Abstr.* **1968**, 69, 58828s. (c) Morita, K.; Suzuki, Z.; Hirose, H. *Bull. Chem. Soc. Jpn.* **1968**, 41, 2815.

(2) (a) Mason, G.; Housseman, C.; Zhu, J. *Angew. Chem., Int. Ed.* **2007**, 46, 4614. (b) Mergott, D. J.; Frank, S. A.; Roush, W. R. *Org. Lett.* **2002**, 4, 3157.

(3) (a) Basaviah, D.; Rao, K. V.; Reddy, R. J. *Chem. Soc. Rev.* **2007**, 36, 1581. (b) Basaviah, D.; Rao, A. J.; Satyanarayana, T. *Chem. Rev.* **2003**, 103, 811. (c) Langer, P. *Angew. Chem., Int. Ed.* **2000**, 39, 3049.

(4) Zhao, G.-L.; Huang, J.-W.; Shi, M. *Org. Lett.* **2003**, 5, 4737. (5) Balan, D.; Adolfsen, H. J. *Org. Chem.* **2001**, 66, 6498. (6) (a) König, C. M.; Harms, K.; Koert, U. *Org. Lett.* **2007**, 9, 4777. (b) Lei, X.; Porco, J. A. Jr. *J. Am. Chem. Soc.* **2006**, 128, 14790.

(7) For synthetic application of Baylis–Hillman adducts see: (a) Singh, V.; Batra, S. *Tetrahedron* **2008**, 64, 4511. (b) Kabalka, G. W.; Venkataiah, B.; Dong, G. *Organometallics* **2005**, 24, 762. (c) Iwabuchi, Y.; Furukawa, M.; Esumi, T.; Hatakeyama, S. *Chem. Commun.* **2001**, 2030.

(8) (a) Shi, Y.-L.; Shi, M. *Eur. J. Org. Chem.* **2007**, 2905. (b) Shi, M.; Xu, Y.-M. *Chem. Commun.* **2001**, 1876. (c) Perlmutter, P.; Teo, C. C. *Tetrahedron Lett.* **1984**, 25, 5951.

(9) (a) Declercq, V.; Martinez, J.; Lamaty, F. *Chem. Rev.* **2009**, 109, 1. (b) Abermil, N.; Masson, G.; Zhu, J. *J. Am. Chem. Soc.* **2008**, 130, 12596. (c) Shi, M.; Qi, M.-J.; Liu, X.-G. *Chem. Commun.* **2008**, 6025. (d) Sorbetti, J. M.; Clary, K. N.; Rankic, D. A.; Wulff, J. E.; Parvez, M.; Back, T. G. *J. Org. Chem.* **2007**, 72, 3326. (e) Gausepohl, R.; Buskens, P.; Kleinen, J.; Bruckmann, A.; Lehmann, C. W.; Klankermayer, J.; Leitner, W. *Angew. Chem., Int. Ed.* **2006**, 45, 3689. (f) Shi, Y.-L.; Shi, M. *Tetrahedron* **2006**, 62, 461. (g) Raheem, I. T.; Jacobsen, E. N. *Adv. Synth. Catal.* **2005**, 347, 1701. (h) Matsui, K.; Takizawa, S.; Sasai, H. *J. Am. Chem. Soc.* **2005**, 127, 3680. (i) Shi, M.; Chen, L.-H.; Li, C.-Q. *J. Am. Chem. Soc.* **2005**, 127, 3790. (j) Xu, Y.-M.; Shi, M. *J. Org. Chem.* **2004**, 69, 417. (k) Kawahara, S.; Nakano, A.; Esumi, T.; Iwabuchi, Y.; Hatakeyama, S. *Org. Lett.* **2003**, 5, 3103.

(10) Early asymmetric version of the traditional Morita–Baylis–Hillman reactions is found to be difficult because of reaction conditions leading to moderate enantiomeric excess. For instance, use of chiral acrylate or chiral C<sub>2</sub>-symmetric catalyst provided low asymmetric induction in the resulting MBH adducts. For example see: (a) McDougal, N. T.; Schaus, S. E. *J. Am. Chem. Soc.* **2003**, 125, 12094. (b) Iwabuchi, Y.; Nakatani, M.; Yokoyama, N.; Hatakeyama, S. *J. Am. Chem. Soc.* **1999**, 121, 10219. (c) Oishi, T.; Oguri, H.; Hirama, M. *Tetrahedron: Asymmetry* **1995**, 6, 1241. (d) Basaviah, D.; Pandiaraju, S.; Sarma, P. K. S. *Tetrahedron Lett.* **1994**, 35, 4227.

(11) (a) Utsumi, N.; Zhang, H.; Tanaka, F.; Barbas, C. F. III. *Angew. Chem., Int. Ed.* **2007**, 46, 1878. (b) Shi, M.; Xu, Y.-M.; Shi, Y.-L. *Chem.—Eur. J.* **2005**, 11, 1794. (c) Shi, M.; Chen, L.-H. *Pure Appl. Chem.* **2005**, 77, 2105. (d) Shi, M.; Chen, L.-H. *Chem. Commun.* **2003**, 1310. (e) Shi, M.; Xu, Y.-M. *Angew. Chem., Int. Ed.* **2002**, 41, 4507.

(12) Roy, D.; Sunoj, R. B. *Org. Lett.* **2007**, 9, 4873.

(13) (a) Faltin, C.; Fleming, E. M.; Connon, S. J. *J. Org. Chem.* **2004**, 69, 6496. (b) Cai, J.; Zhou, Z.; Zhao, G.; Tang, C. *Org. Lett.* **2002**, 4, 4723. (c) Yu, C. Z.; Liu, B.; Hu, L. Q. *J. Org. Chem.* **2001**, 66, 5413. (d) Auge, J.; Lubin, N.; Lubineau, A. *Tetrahedron Lett.* **1994**, 35, 7947.

(14) (a) Bode, M. L.; Kaye, P. T. *Tetrahedron Lett.* **1991**, 32, 5611. (b) Hill, J. S.; Isaacs, N. S. *J. Phys. Org. Chem.* **1990**, 3, 285.

(15) (a) Amarante, G. W.; Milagre, H. M. S.; Vaz, B. C.; Ferreira, B. R. V.; Eberlin, M. N.; Coelho, F. *J. Org. Chem.* **2009**, 74, 3031. (b) Krafft, M. E.; Haxell, T. F. N.; Seibert, K. A.; Abboud, K. A. *J. Am. Chem. Soc.* **2006**, 128, 4174. (c) Santos, L. S.; Pavam, C. H.; Almeida, W. P.; Coelho, F.; Eberlin, M. N. *Angew. Chem., Int. Ed.* **2004**, 43, 4330.

(16) Price, K. E.; Broadwater, S. J.; Walker, B. J.; McQuade, D. T. *J. Org. Chem.* **2005**, 70, 3980.

lesser significance than the primary hydrogen bonding stabilization offered by protic cosolvents.<sup>17</sup>

In a very recent report from our group, the role of water in the NMe<sub>3</sub>-catalyzed MBH reaction between acrolein and formaldehyde was illustrated.<sup>18</sup> The most prominent role of water molecule(s) is identified as helping an intramolecular proton transfer through a relay mechanism. It was identified that the effective participation of the water molecule and the accompanying reduction in the activation barrier for the proton transfer process makes the C–C bond formation step energetically competitive to be the RDS. We have also noted that water molecule(s) residing away from the reaction coordinate do not have a significant role on the reaction energetics. In another study, methanol-assisted proton transfer in the NMe<sub>3</sub>-catalyzed MBH reaction between methylacrylate and benzaldehyde was reported.<sup>19</sup> These reports indeed allude to the possibility of an analogous role of polar protic solvent/additive in the mechanism of the aza-MBH reaction as in the case of the MBH reaction.<sup>20</sup>

Though there are mechanistic similarities between the commonly employed electrophiles such as aldehyde and imines, reports are also available that bring out the difference between these electrophiles.<sup>2a,8a,11c</sup> Further, the reaction profile could vary depending on the presence or absence of protic cocatalysts. Such studies focusing on aza-MBH reaction are not reported until now. In this paper, we intend to report the first computational study directed toward unraveling the role of protic cocatalysts on the mechanism of the aza-MBH reaction. The key transition states with explicitly included water molecule(s) are examined. Apart from water, other protic additives such as methanol and formic acid are also considered to probe their potential role in rate-acceleration of the aza-MBH reaction.

## Computational Methods

All calculations were performed with the Gaussian03 suite of quantum chemical programs.<sup>21</sup> Full geometry optimizations followed by frequency calculations on all the stationary points were carried out to ascertain the nature of the stationary points as a minimum or a transition state on the potential energy surface. All the transition states were characterized by one and only one imaginary frequency pertaining to the desired reaction coordinate. The intrinsic reaction coordinate (IRC) calculations were carried out at the mPW1K level to further authenticate the transition states.<sup>22</sup> We have employed the hybrid density functional method, mPW1K, in combination with the 6-31+G\*\* basis set in this study.<sup>23</sup> The choice of the density functional mPW1K (consisting of 42.8% HF mixing) is based on its successful applications in predicting reliable activation parameters.<sup>12,18,24</sup>

Additionally, the complete basis set extrapolation method using composite ab initio methods such as CBS-4M is employed to further refine the computed activation parameters.<sup>25</sup> The final geometries obtained at the end of the IRC path on both sides of the first-order saddle points were then subjected to further geometry optimization by using stringent optimization conditions with the “Opt = calcfc” option. This will enable a careful *walk down* from the final IRC point along the PES. The Gibbs free energies in the gas phase were obtained by including zero-point vibrational energy (ZPVE) as well as thermal corrections to the *bottom-of-the-well* values. The reported gas-phase relative energies (represented as  $\Delta E$  for all the transition states) are inclusive of ZPVE, while those obtained by using the single-point energy calculations in a dielectric continuum refer to the *bottom-of-the-well* values. All barriers described in this report are with reference to separated reactants, unless otherwise specified.

To examine the effect of basis sets on the computed barriers, two key steps in the reaction sequence, namely the C–C bond formation and intramolecular proton transfer, are reoptimized at the mPW1K level by using more flexible 6-311+G\*\*, cc-pVDZ, cc-pVTZ, and aug-cc-pVDZ basis sets.<sup>26</sup>

Further, the effect of solvation is incorporated through single-point energy calculations by using the integral equation formalism (IEF) within the polarized continuum model (PCM) framework with UAKS radii.<sup>27</sup> We have performed these calculations at the IEF-PCM/mPW1K/6-31+G\*\*//mPW1K/6-31+G\*\* level of theory.<sup>28</sup> Three commonly used solvents in the aza-MBH reaction were chosen for the present study. These are THF ( $\epsilon = 7.6$ ), DMSO ( $\epsilon = 46.7$ ), and water ( $\epsilon = 78.4$ ).

The global electrophilicity indices ( $\omega$ ) are calculated by using the following equation,  $\omega = \mu^2/2\eta$ , where  $\mu$  and  $\eta$  denote electronic chemical potential and chemical hardness, respectively.<sup>29</sup> Both these quantities ( $\mu$  and  $\eta$ ) are calculated by using the following expressions:  $\mu \approx (\epsilon_{\text{HOMO}} + \epsilon_{\text{LUMO}})/2$  and  $\eta \approx (\epsilon_{\text{LUMO}} - \epsilon_{\text{HOMO}})/2$ , where  $\epsilon_{\text{HOMO}}$  and  $\epsilon_{\text{LUMO}}$  are energies of the frontier orbitals HOMO and LUMO, respectively.<sup>30</sup>

## Results and Discussion

The aza-MBH reaction between mesyl imine (derived from formaldehyde) and acrolein, catalyzed either by trimethylamine (NMe<sub>3</sub>) or trimethylphosphine (PMe<sub>3</sub>), is studied by using the mPW1K and CBS-4M levels of theories. The discussions primarily focus on (i) the likely nature of the

(17) Aggarwal, V. K.; Dean, D. K.; Mereu, A.; Williams, R. *J. Org. Chem.* **2002**, *67*, 510.

(18) Roy, D.; Sunoj, R. B. *Chem.—Eur. J.* **2008**, *34*, 10530.

(19) Robiette, R.; Aggarwal, V. K.; Harvey, J. N. *J. Am. Chem. Soc.* **2007**, *129*, 15513.

(20) Aggarwal, V. K.; Fulford, S. Y.; Lloyd-Jones, G. C. *Angew. Chem., Int. Ed.* **2005**, *44*, 1706.

(21) Frisch et al. *Gaussian 03*, revision C.02; Gaussian, Inc.: Wallingford, CT, 2004. (See the Supporting Information for the full citation.)

(22) Gonzalez, C.; Schlegel, H. B. *J. Chem. Phys.* **1989**, *90*, 2154.

(23) (a) Lynch, B. J.; Fast, P. L.; Harris, M.; Truhlar, D. G. *J. Phys. Chem. A* **2000**, *104*, 4811. (b) Lynch, B. J.; Zhao, Y.; Truhlar, D. G. *J. Phys. Chem. A* **2003**, *107*, 1384.

(24) (a) Seckute, J.; Menke, J. L.; Emmett, R. J.; Patterson, E. V.; Cramer, C. J. *J. Org. Chem.* **2005**, *70*, 8649. (b) Lingwood, M.; Hammond, J. R.; Hrovat, D. A.; Mayer, J. M.; Borden, W. T. *J. Chem. Theory Comput.* **2006**, *2*, 740.

(25) (a) Ochterski, J. W.; Petersson, G. A.; Montgomery, J. A. Jr. *J. Chem. Phys.* **1996**, *104*, 2598. (b) Montgomery, J. A. Jr.; Frisch, M. J.; Ochterski, J. W.; Petersson, G. A. *J. Chem. Phys.* **2000**, *112*, 6532.

(26) (a) Woon, D. E.; Dunning, T. H. Jr. *J. Chem. Phys.* **1993**, *98*, 1358. (b) Kendall, R. A.; Dunning, T. H. Jr.; Harrison, R. J. *J. Chem. Phys.* **1992**, *96*, 6796.

(27) (a) Cancès, M. T.; Mennucci, B.; Tomasi, J. *J. Chem. Phys.* **1997**, *107*, 3032. (b) Mennucci, B.; Tomasi, J. *J. Chem. Phys.* **1997**, *106*, 5151. (c) Mennucci, B.; Cancès, E.; Tomasi, J. *J. Phys. Chem. B* **1997**, *101*, 10506. (d) Tomasi, J.; Mennucci, B.; Cancès, E. *J. Mol. Struct.: THEOCHEM* **1999**, *464*, 211.

(28) The entropic contributions of the solute evaluated with the help of the gas-phase frequency calculation are not quite good toward the application to a solute in a continuum dielectric (Leung, B. O.; Reid, D. L.; Armstrong, D. A.; Rauk, A. *J. Phys. Chem. A* **2004**, *108*, 2720). However, the use of single-point energies in solvent continuum is a widely adopted method toward gauging the role of solvent continuum in chemical reactions. Some very recent examples include: (a) Schoenebeck, F.; Houk, K. N. *J. Org. Chem.* **2009**, *74*, 1464. (b) Domingo, L. R.; Picher, M. T.; Sáez, J. A. *J. Org. Chem.* **2009**, *74*, 2726. (c) Brookes, N. J.; Ariafard, A.; Stranger, R.; Yates, B. F. *J. Am. Chem. Soc.* **2009**, *131*, 5800.

(29) Parr, R. G.; von Szentpaly, L.; Liu, S. *J. Am. Chem. Soc.* **1999**, *121*, 1922.

(30) (a) Parr, R. G.; Pearson, R. G. *J. Am. Chem. Soc.* **1983**, *105*, 7512. (b) Parr, R. G.; Yang, W. *Density Functional Theory of Atoms and Molecules*; Oxford University Press: New York, 1989.



**TABLE 1. The Relative Energies<sup>a</sup> (in kcal/mol) of the C–C Bond Formation and Proton Transfer Transition States Involved in the NMe<sub>3</sub>-Catalyzed Aza-MBH Reaction between Acrolein and Mesityl Imine**

TS	CBS-4M		mPW1K/6-31 + G**					
	$\Delta E$	$\Delta G$	$\Delta E$	$\Delta G$	$\Delta E_{(\text{THF})}^b$	$\Delta E_{(\text{DMSO})}^b$	$\Delta E_{(\text{water})}^b$	
<b>1a–1b</b>	9.2	22.1	10.0	22.3	4.2	3.5	1.6	
<b>1b–1c</b>	7.6	34.0	11.8	37.7	4.7	4.4	1.8	
<b>1c–1d</b>	20.9	45.7	24.0	49.0	10.3	8.4	3.3	
<b>1d–1e</b>	-15.8	9.3	-15.8	7.7	-22.0	-22.3	-26.6	

<sup>a</sup>The relative energies are computed with respect to the infinitely separated reactants. <sup>b</sup>The single-point energies are at the IEF-PCM<sub>(solvent)</sub>/mPW1K/6-31 + G\*\* level on the gas-phase optimized geometries.

rate-limiting step, (ii) the influence of explicitly included solvent/cocatalyst molecule(s) on the reaction profile, and (iii) comparison with the parent MBH reaction as well as between cocatalyst-assisted and unassisted pathways.

In the first step of the aza-MBH reaction, a zwitterionic intermediate (**1b**) is generated by the addition of NMe<sub>3</sub> to acrolein. In the next step, the C–C bond formation through the addition of **1b** to mesityl imine results in intermediate **1c**. An intramolecular proton transfer via a four-membered transition state (**TS(1c–1d)**) is the next key step. The calculated relative energies of the transition states for four important steps in the reaction sequence are provided in Table 1. The relative Gibbs free energies of the transition state for the proton transfer step are found to be much larger than those of the preceding elementary steps, indicating that the proton transfer could act as the rate-determining step in the gas phase. Additional analysis on the basis of the computed barriers with respect to the respective prereacting complexes or intermediates further supports this view.<sup>31</sup> It is noteworthy that the relative energies obtained at the mPW1K and CBS-4M levels are in good mutual agreement. Further, the computed energetics obtained by using Pople's basis set 6-31 + G\*\* are found to be quite consistent with those calculated with Dunning's correlation consistent basis sets.<sup>32</sup> On the basis of these observations, we have chosen the mPW1K functional in conjunction with the 6-31 + G\*\* basis set for the present study. The optimized geometries of the transition states for the C–C bond formation and intramolecular proton transfer in the NMe<sub>3</sub>-catalyzed aza-MBH reaction are provided in Figure 1.

Since the reaction proceeds through several charge-separated polar intermediates, we have examined the role of continuum solvation using the gas-phase geometries (Table 1). The incorporation of solvent effects with the help of single-point energy calculations at the mPW1K/6-31 + G\*\* level indicates an overall decrease in the activation energies in all three solvents considered herein. A closer inspection of the relative energies of the transition states in the condensed phase reveals some interesting features. Firstly, among the four elementary steps of the aza-MBH reaction, the C–C bond formation and the proton transfer are found to exhibit larger solvent effects. For instance, the stabilization is

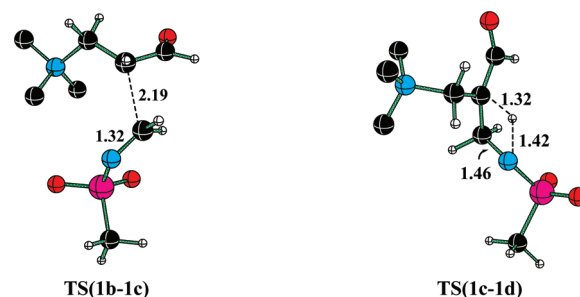


**FIGURE 1.** The mPW1K/6-31 + G\*\* optimized geometries of key transition states involved in the NMe<sub>3</sub>-catalyzed aza-MBH reaction between acrolein and mesityl imine. Only select hydrogens are shown for improved clarity. [Atom color code: black, C; cyan, N; red, O; pink, S; and ivory, H. Bond lengths are in Å.]

found to be of the order of 10 and 21 kcal/mol, respectively, for the C–C bond formation and proton transfer in water continuum.<sup>33</sup> This can be attributed to a relatively higher charge separation or increased polarity of the corresponding transition states.<sup>34</sup> Further, the most polar solvent considered here (water) offers maximum stabilization as evident from the computed energy parameters of the transition states. It is of significance to note that even after the inclusion of solvent effects through implicit models the overall conclusions as derived from the gas-phase calculations continue to remain the same.<sup>35</sup>

The computed relative energies of the key transition states for the PMe<sub>3</sub>-catalyzed reaction are provided in Table 2.<sup>36</sup> While the general mechanistic features are quite similar to that with the NMe<sub>3</sub>-catalyzed reaction, the relative energy of the transition state for the C–C bond formation step is found to be noticeably lower. The kinetic advantage of the PMe<sub>3</sub>-catalyzed reaction is also evident in the proton transfer step, where the energies of the transition states are much lower than those of the corresponding NMe<sub>3</sub>-catalyzed reaction. These predictions are consistent with the available experimental reports where faster reaction rates are in general noticed for the phosphine-catalyzed aza-MBH reaction.<sup>9h,37</sup>

The available experimental reports as well as the involvement of polar intermediates in aza-MBH evidently suggest that under polar protic conditions the mechanistic course could be different from that under aprotic conditions. Interesting experiments on rate enhancements in the presence

(34) Although the relative energies computed by using the separated reactants, as the reference point, are negative, those with respect to the preceding prereacting complex (PRC) or intermediate are found to be positive (see Table S6, Supporting Information). This feature arises due to the improved stabilization of the charged intermediates in polar solvents (dielectric continuum). See Table S7 in the Supporting Information for  $G_{\text{solvation}}$  of the intermediates involved in the NMe<sub>3</sub>-catalyzed reaction.

(35) To examine the role of solvent continuum in the aza-MBH reaction arising as a result of the likely differences in the geometries between the gas phase and the condensed phase, we have additionally carried out geometry optimizations using THF as a representative solvent continuum. The results are summarized in Table S8 in the Supporting Information. Interestingly, the single-point energies calculated in the continuum dielectric medium by using the gas-phase geometries are found to be nearly identical. The same trends were reproduced by full geometry optimizations in the THF dielectric continuum.

(36) The barrier for the formation of the *E*-isomer of **2b** is found to be about 5 kcal/mol higher than that for the corresponding *Z*-isomer.

(37) The relatively higher activity of the phosphorous-containing Lewis bases in the aza-MBH reaction can partially be attributed to the ease of accommodating a positive charge on a phosphorous as compared to that on a nitrogen atom.

(31) See Table S6 in the Supporting Information for further details.

(32) More details on the choice of basis set as well as the computed activation parameters obtained by using different basis sets (such as 6-311+G\*\*, cc-pVDZ, cc-pVTZ, and aug-cc-pVDZ) are provided in Table S5 in the Supporting Information.

(33) These are differences between the energies of the transition states, as given by  $E_{\text{gas}}$  and  $E_{\text{water}}$ .

**TABLE 2.** The Relative Energies<sup>a</sup> (in kcal/mol) for the C–C Bond Formation and Proton Transfer Steps Involved in the PMe<sub>3</sub>-Catalyzed Aza-MBH Reaction between Acrolein and Mesityl Imine

TS	CBS-4M		mPW1K/6-31+G**				
	$\Delta E$	$\Delta G$	$\Delta E$	$\Delta G$	$\Delta E_{(\text{THF})}^b$	$\Delta E_{(\text{DMSO})}^b$	$\Delta E_{(\text{water})}^b$
2a–2b	9.5	21.5	9.4	20.9	8.1	7.8	7.2
2b–2c	–15.8 <sup>c</sup>	10.1	–1.4	23.9	–3.3	–3.3	–4.6
2c–2d	8.1	31.8	9.5	33.6	1.5	0.3	–4.2
2d–2e	–17.4	5.2	–17.7	5.8	–21.3	–21.4	–24.8

<sup>a</sup>The relative energies are computed with respect to the infinitely separated reactants. <sup>b</sup>The single-point energies are at the IEF-PCM<sub>(solvent)</sub>/mPW1K/6-31+G\*\* level on the gas-phase optimized geometries. <sup>c</sup>The large difference between CBS-4M and mPW1K values for TS(2b–2c) is identified as arising due to the differences in the geometrical features.

of polar protic cocatalysts for both MBH and aza-MBH reactions are also reported.<sup>13</sup> In the context of the present study, we propose a direct involvement of polar protic cocatalyst in the reaction. Explicit inclusion of cocatalyst in the critical transition state models is therefore considered. Such an approach could have a direct effect on the reaction coordinate and the associated energetics. There are interesting recent examples on the role of polar protic cocatalysts such as water and methanol toward reducing the activation barriers through relay proton transfer mechanisms in several other reactions.<sup>38</sup> The effect of three such cocatalysts, namely water, methanol, and formaldehyde, is examined in the present study.

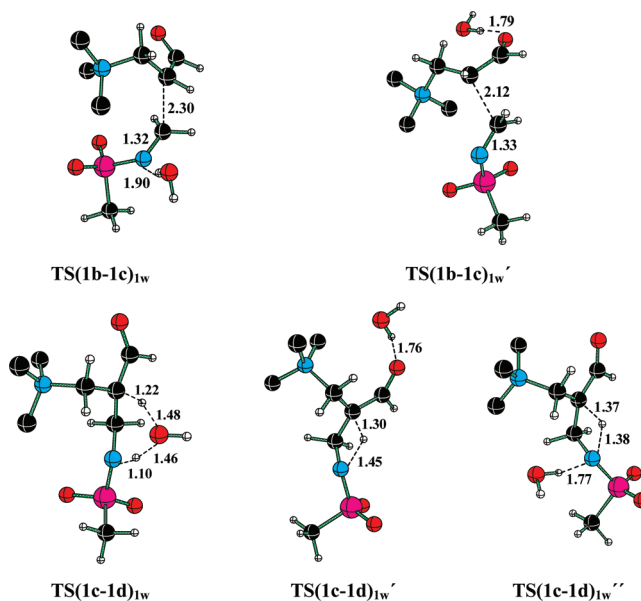
To begin with, one water molecule is incorporated with the electrophile through the imino nitrogen. This kind of water coordination is considered first, as the developing negative charge in the C–C bond formation transition state is expected to enjoy an improved stabilization. Further, in an earlier study we have established that the coordination of protic solvents to the electrophile is energetically more effective as compared to that with the nucleophile or other reactant(s).<sup>12,18</sup> While the explicit water molecule can alternatively be considered as interacting with the sulfonyl oxygen(s), noticeable lowering of reaction barriers is highly likely when the developing negative charge on the imino nitrogen is stabilized by the explicit water molecule (vide infra).<sup>39</sup> The interaction energy of the water molecule with mesityl imine is estimated to be 4.8 kcal/mol at the mPW1K/6-31+G\*\* level of theory.<sup>40</sup>

Consideration of water-bound transition states brings out some interesting mechanistic features of the aza-MBH reaction. The computed relative energies of the transition states for different elementary steps for the NMe<sub>3</sub>-catalyzed reaction are summarized in Table 3. The C–C bond formation transition state with one bound water, represented as TS-(1b–1c)<sub>1w</sub>, is found to be enthalpically more stable than the corresponding unassisted transition state, TS(1b–1c) (Figure 2). However, the gas-phase Gibbs free energies of

**TABLE 3.** The Relative Energies<sup>a</sup> (in kcal/mol) for the C–C Bond Formation and Proton Transfer Steps Involved in the Water-Assisted Aza-MBH Reaction between Acrolein and Mesityl Imine Catalyzed by NMe<sub>3</sub>

mode	TS	CBS-4M		mPW1K/6-31+G**				
		$\Delta E$	$\Delta G$	$\Delta E$	$\Delta G$	$\Delta E_{(\text{THF})}^b$	$\Delta E_{(\text{DMSO})}^b$	$\Delta E_{(\text{water})}^b$
1w <sup>c</sup>	1b–1c	3.2	38.4	4.8	38.1	1.7	2.2	1.9
	1c–1d	–3.2	33.1	–3.9	31.7	–10.0	–10.0	–10.7
1w'	1b–1c	–0.5	35.3	2.2	37.4	–2.2	–1.6	–1.1
	1c–1d	12.0	46.4	13.4	47.4	2.9	2.1	0.1
1w''	1b–1c	3.2	38.4	4.8	38.1	1.7	2.2	1.9
	1c–1d	8.6	43.6	9.8	44.2	2.5	2.1	1.2

<sup>a</sup>The relative energies are computed with respect to the infinitely separated reactants. <sup>b</sup>The single-point energies are at the IEF-PCM<sub>(solvent)</sub>/mPW1K/6-31+G\*\* level on the gas-phase optimized geometries. <sup>c</sup>TS(1b–1c) is the same for both 1w and 1w'' modes.

**FIGURE 2.** The mPW1K/6-31+G\*\* optimized geometries of the transition states for the one-water-assisted NMe<sub>3</sub>-catalyzed aza-MBH reaction between acrolein and mesityl imine. Only select hydrogens are shown for improved clarity. [Atom color code: black, C; cyan, N; red, O; pink, S; and ivory, H. Bond lengths are in Å.]

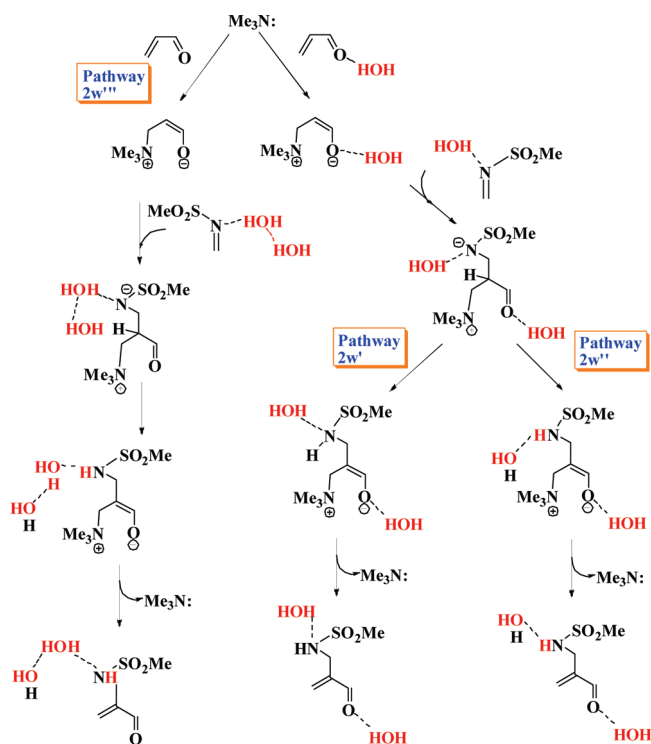
the transition states computed at the CBS-4M level for both water-assisted and unassisted modes of C–C bond formation are found to be similar. Improved stabilization of the water-bound transition states is more evident with the inclusion of continuum solvation effects. The lower energies of the transition states for the C–C bond formation in the water-assisted mode arise primarily due to the stabilization of the developing charges, besides the LUMO stabilization of the electrophile offered by the coordinated water molecule.<sup>41</sup> In the second key step, this explicit water molecule could facilitate a relay proton transfer through a cyclic six-membered chairlike transition state, as depicted in TS-(1c–1d)<sub>1w</sub> in Figure 2. The relative Gibbs free energy for this water-assisted proton transfer transition state is lower by about 17 kcal/mol than the corresponding unassisted mode at the mPW1K level of theory. The subsequent expulsion of

(38) (a) Patil, M. P.; Sunoj, R. B. *Chem.—Eur. J.* **2008**, *14*, 10472. (b) Tian, Z.; Kass, S. R. *J. Am. Chem. Soc.* **2008**, *130*, 10842. (c) Patil, M. P.; Sunoj, R. B. *J. Org. Chem.* **2007**, *72*, 8202. (d) Vilotijevic, I.; Jamison, T. F. *Science* **2007**, *317*, 1189. (e) Lundin, A.; Panas, I.; Ahlberg, E. *J. Phys. Chem. A* **2007**, *111*, 9087. (f) Shi, F.-Q.; Li, X.; Xia, Y.; Zhang, L.; Yu, Z.-X. *J. Am. Chem. Soc.* **2007**, *129*, 15503. (g) Xia, Y.; Liang, Y.; Chen, Y.; Wang, M.; Jiao, L.; Huang, F.; Liu, S.; Li, Y.; Yu, Z.-X. *J. Am. Chem. Soc.* **2007**, *129*, 3470.

(39) For comparison of Mulliken atomic charges in TS(1b–1c) and 1c see Figure S2 in the Supporting Information.

(40) Interaction energy ( $\Delta H$ ) is calculated without the basis set superposition error (BSSE) correction.

(41) The computed LUMO energies of bare and water-bound mesityl imines are respectively found to be –0.040 and –0.049 eV at the mPW1K/6-31+G\*\* level of theory. See Table S9 in the Supporting Information.

**SCHEME 2. Important Modes of Participation by Two Water Molecules in the Aza-MBH Reaction between MVK and Mesityl Imine<sup>a</sup>**


<sup>a</sup>Explicitly included water molecules are shown in red.

NMe<sub>3</sub> is found to be of comparable barrier as that of the unassisted TS(1d–1e), implying a less pronounced effect of the specific interaction with water in the last step.<sup>42</sup>

The alternative modes of stabilization of the key transition states are also considered. In these transition states TS-(1b–1c)<sub>1w'</sub> and TS(1c–1d)<sub>1w''</sub>, the explicit water molecule is bound respectively to the enolate and mesityl imine fragments. The incipient charges in these TSs are more effectively stabilized as compared to that in the unassisted pathway as shown in Figure 2. Interestingly, the proton transfer in TS(1c–1d)<sub>1w</sub> involving a relay mechanism is identified as more efficient than that in TS(1c–1d)<sub>1w''</sub>. In the former case, both electrostatic stabilization and reduced strain in the cyclic six-membered TS geometry offer improved stabilization, whereas in the later situation, charge stabilization is identified as the major contribution by the bound water molecule. Similar features are also noticed for the water-assisted PMe<sub>3</sub>-catalyzed aza-MBH reaction.<sup>43</sup>

As a logical extension toward identifying improved transition state models for the solvent-assisted pathways, we have incorporated two water molecules in the NMe<sub>3</sub>-catalyzed aza-MBH reaction. While the possible coordination modes

(42) The relative energies for the elimination step are provided in Table S10 in the Supporting Information.

(43) See Table S11 in the Supporting Information for the relative energies associated with the one water-assisted, PMe<sub>3</sub>-catalyzed aza-MBH reaction.

(44) We have also been able to locate other near-degenerate transition states for the C–C bond formation with different spatial dispositions of the two water molecules than those discussed here. However, all such transition states are found to be of higher energies than that for the 2w' mode. See Table S12 and Figure S1 in the Supporting Information for more details.

**TABLE 4. The Relative Energies<sup>a</sup> (in kcal/mol) for the C–C Bond Formation and Proton Transfer Steps Involved in the Two-Water-Assisted Aza-MBH Reaction between Acrolein and Mesityl Imine Catalyzed by NMe<sub>3</sub>**

mode	TS	CBS-4M		mPW1K/6-31+G**				
		$\Delta E$	$\Delta G$	$\Delta E$	$\Delta G$	$\Delta E_{(\text{THF})}$ <sup>b</sup>	$\Delta E_{(\text{DMSO})}$ <sup>b</sup>	$\Delta E_{(\text{water})}$ <sup>b</sup>
2w'	1b–1c	–4.0	39.9	–5.1	37.5	–5.4	–3.8	–0.2
	1c–1d	–0.2	44.4	–0.5	42.8	–4.2	–3.5	–1.2
2w''	1c–1d	–11.7	33.9	–13.5	30.8	–16.6	–15.8	–13.8
	1b–1c	–4.8	39.4	–5.8	37.4	–4.9	–3.1	1.3
2w'''	1b–1c	–4.8	39.4	–5.8	37.4	–4.9	–3.1	1.3
	1c–1d	–17.8	29.1	–16.5	28.0	–19.4	–18.5	–16.3

<sup>a</sup>The relative energies are computed with respect to the infinitely separated reactants. <sup>b</sup>The single-point energies are at the IEF-PCM<sub>(solvent)</sub>/mPW1K/6-31+G\*\* level on the gas-phase optimized geometries.

are expected to be larger, only three key possibilities as represented in Scheme 2 are considered here.<sup>44</sup> Two of these modes involve binding of one water molecule each with the enolate and mesityl imine. In the other possibility both water molecules bind to mesityl imine. In pathway 2w', stabilizing hydrogen bonding interactions with the developing charge at the nitrogen of mesityl imine and oxygen of the enolate moiety are likely. In pathways 2w'' and 2w''', one or both water molecules are involved in a relay proton transfer.

The relative energies of various transition states for the above-mentioned pathways with two water molecules are summarized in Table 4. Evidently, modes 2w'' and 2w''' involving the relay proton transfer are more effective in stabilizing the transition states than that with predominant electrostatic interactions (viz., 2w'). For instance, the comparison of Gibbs free energies of the transition states reveals that 2w''' exhibits the lowest energy for the proton transfer. Such participation by two bound water molecules in the proton transfer step is identified as so effective that the relative energies of the corresponding transition states are found to be lower than that for the C–C bond formation. A similar feature is also noticed for the 2w'' mode where only one of the water molecules facilitates the relay proton transfer, while the other interacts with the enolate moiety. The two water-assisted modes convey that as the efficiency of proton transfer mediated by the bound water molecule(s) increases, the energy difference between the C–C bond formation and the proton transfer transition states becomes progressively lower. Interestingly, the trends in the relative energies of the transition states obtained in the gas phase are found to remain the same in the condensed phase computed by using the continuum solvation model. The important geometrical parameters of the transition states for two water-assisted C–C bond formation as well as proton transfer are summarized in Figure 3.

A number of recent experimental reports suggest that the use of polar protic additives such as methanol, phenol, and carboxylic acids could offer rate acceleration in the MBH reaction. In fact, Leitner and co-workers reported that the rate acceleration in the PPh<sub>3</sub>-catalyzed aza-MBH reaction is found to be the highest in which phenolic additives/cocatalysts are employed.<sup>45</sup> They have concluded that in the absence of protic additives, the RDS in the aza-MBH reaction is the proton transfer.<sup>46</sup> To probe the role of

(45) Buskens, P.; Klankermayer, J.; Leitner, W. *J. Am. Chem. Soc.* **2005**, *127*, 16762.

(46) However, the possible role of protic additives with small pK<sub>a</sub> values toward protonation of the zwitterionic intermediates or the base is suggested as capable of slowing down the reaction rates.



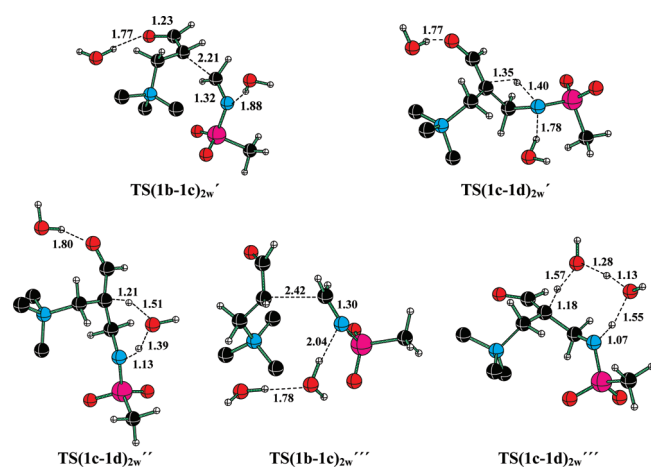


**FIGURE 3.** The mPW1K/6-31+G\*\* optimized geometries of the C–C bond formation and proton transfer transition states for two-water-assisted NMe<sub>3</sub>-catalyzed aza-MBH reaction between acrolein and mesyl imine. Only select hydrogens are shown for improved clarity. [Atom color code: black, C; cyan, N; red, O; pink, S; and ivory, H. Bond lengths are in Å.]

nonaqueous cocatalysts in the aza-MBH reaction, we have examined the C–C bond formation as well as the proton transfer steps in the NMe<sub>3</sub>-catalyzed aza-MBH reaction with explicitly included cocatalysts. The transition state models with bound protic cocatalysts, such as methanol or formic acid, are located at the mPW1K/6-31+G\*\* level of theory.

The computed relative energies of the transition states for two key steps are provided in Table 5. Noticeably, the relative Gibbs free energy for the C–C bond formation in the gas phase shows a smaller difference relative to the unassisted pathway upon inclusion of cocatalysts of varying p*K*<sub>a</sub> values.<sup>47</sup> The difference in the relative free energies for the C–C bond formation with and without the cocatalyst is only about 4 kcal/mol. The optimized transition state geometries reveal that the reaction coordinate remains quite similar in all three cases when the cocatalyst is bound to the nitrogen of mesyl imine (see Figures 2 and 4). The closely related C–C bond formation barriers for these three cocatalysts can be rationalized on the basis of (i) the stabilization of the LUMO of the cocatalyst-bound electrophile and (ii) global electrophilicity indices.<sup>48</sup> These predictions allude to a more vital role of protic cocatalyst in the proton transfer as compared to that in the C–C bond formation.

Indeed, the energetics of the relay proton transfer exhibits a profound effect with respect to the nature of the cocatalyst. The lowest energy transition state for the proton transfer step is noticed for formic acid-assisted relay proton transfer. The reaction coordinates for the water- or methanol-assisted proton transfer are found to be quite similar while a larger difference is noticed for that with formic acid (Figures 2 and 4). In the case of formic acid, delivery of the proton to the imino nitrogen is found to be ahead of its abstraction. This

(47) The p*K*<sub>a</sub> values for water, methanol, and formic acid are respectively 15.4, 15.5, and 3.7.

(48) (a) The LUMO energies of water/methanol/formic acid-bound mesyl imine are quite comparable; e.g., water (−0.049), MeOH (−0.049), and formic acid (−0.051). (b) Additionally, the global electrophilicity indices for the cocatalyst-bound imines are estimated to be quite similar as well. See Table S9 in the Supporting Information for global electrophilicity indices of electrophiles employed in this study.

**TABLE 5.** The Relative Energies<sup>a</sup> (in kcal/mol) for the C–C Bond Formation and Proton Transfer Transition States in the NMe<sub>3</sub>-Catalyzed Aza-MBH Reaction with Various Cocatalysts<sup>b</sup>

cocatalyst	TS	Δ <i>E</i>	Δ <i>G</i>	Δ <i>E</i> <sub>(THF)</sub> <sup>c</sup>	Δ <i>E</i> <sub>(DMSO)</sub> <sup>c</sup>	Δ <i>E</i> <sub>(water)</sub> <sup>c</sup>
MeOH	(1b–1c)	4.4	38.9	3.0	3.7	3.8
	(1c–1d)	−5.4	31.2	−9.5	−9.5	−10.5
HCO <sub>2</sub> H	(1b–1c)	−0.7	35.4	−1.8	−1.2	0.2
	(1c–1d)	−25.6	11.8	−26.9	−26.4	−24.9
	(1c–1d) <sup>e</sup>	−18.5	18.2	−23.3	−23.5	−23.8

<sup>a</sup>Calculated with reference to the infinitely separated reactants at the mPW1K/6-31+G\*\* level of theory. <sup>b</sup>The corresponding values for the unassisted and water-assisted pathways are respectively provided in Tables 1 and 3. <sup>c</sup>The single-point energies are at the IEF-PCM<sub>(solvent)/mPW1K/6-31+G\*\* level on the gas-phase optimized geometries.</sub>

delayed relay can be attributed to the higher acidity of formic acid as compared to the other additives.<sup>49</sup> A concomitant proton abstraction by the ensuing formate ion then follows as shown in Figure 4. The mode in which both the oxygen atoms of the formic acid participate in relay proton transfer, depicted as TS(1c–1d)<sub>formic</sub>, is relatively more efficient. The Gibbs free energy for another mode TS(1c–1d)<sub>formic</sub>, where only one of the oxygen atoms is involved in the proton transfer, is found to be more than 6 kcal/mol higher. These predictions suggest that the aza-MBH reaction could enjoy the benefits of relay proton transfer promoted by polar protic cosolvents and therefore could offer rate enhancements.

It is interesting to compare the mechanistic features of the aza-MBH reaction with those of the MBH reaction at this juncture. The overall reaction profile of the NMe<sub>3</sub>- or PMe<sub>3</sub>-catalyzed aza-MBH reaction appears similar to that of the MBH reaction with a related set of substrates.<sup>50</sup> The activated imines employed in the aza-MBH reaction are evidently more electrophilic than the corresponding aldehydes in the MBH reaction.<sup>51</sup> As a result, the energy of the C–C bond formation transition state in the aza-MBH reaction is in general slightly lower than that for the MBH reaction. A more striking difference is noticed in the intramolecular proton transfer step. The relative energy for the proton transfer transition state in the aza-MBH reaction is found to be much lower as compared to that of the MBH reaction.<sup>52</sup> This can be attributed to the higher negative charge on the imino nitrogen attached to an electron withdrawing group as well as the relatively lower strain in the transition state geometry for the aza-MBH reaction.<sup>53</sup> The key mechanistic similarity is with the relative energies of the proton transfer transition states. Under aprotic conditions, the intramolecular proton transfer transition state is identified to occupy the highest energy point

(49) Calculated bond orders further support the geometric features of these transition states. See Table S13 in the Supporting Information for more details of the NBO analysis on the cocatalyst-assisted proton transfer transition state TS(1c–1d).

(50) See Figures S4 and S5 in the Supporting Information for the optimized geometries of the transition states respectively for the PMe<sub>3</sub>-catalyzed aza-MBH reaction and the corresponding MBH reaction.

(51) See Table S9 in the Supporting Information for global electrophilicity indices of electrophiles (with and without the bound cocatalysts) considered in this study.

(52) See Table S15 in the Supporting Information for a summary of relative energies for the corresponding transition states for the MBH reaction.

(53) In the cyclic four-membered transition state for the unassisted proton transfer, the C–N distance in mesyl imine (aza-MBH) is longer than the C–O distance (MBH). See Table S14 in the Supporting Information for a comparative analysis of the key geometrical features of TS(1c–1d).

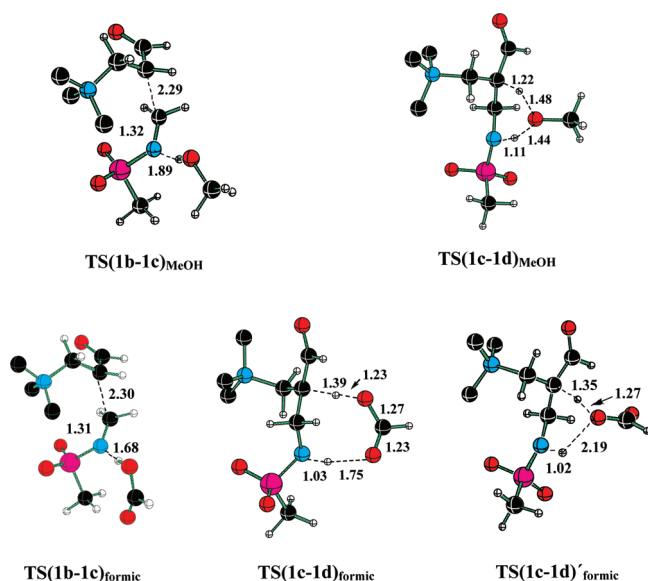


**FIGURE 4.** The mPW1K/6-31+G\*\* optimized geometries of the transition states of the cocatalyst-assisted pathways in the aza-MBH reaction. Only select hydrogens are shown for improved clarity. [Atom color code: black, C; cyan, N; red, O; pink, S; and ivory, H. Bond lengths are in Å.]

on the potential energy surface in both these reactions. In the presence of protic cocatalysts, diminishing energy differences between the transition states for the C–C bond formation and the proton transfer are noticed.<sup>54,55</sup> The situation is found to be interestingly different when formic acid facilitates the relay proton transfer. Due to the improved efficiency of formic acid-mediated proton transfer, the transition state for proton transfer enjoys better stabilization than that for the C–C bond formation. Similar features are also evident in the water-assisted relay proton transfer (**1w**, **2w''**, **2w'''**) in the aza-MBH reaction. However, the nature of the rate-determining step will be affected by the relative stabilities of the preceding intermediates involved in the C–C bond formation and the proton transfer steps. We have identified such intermediates for the NMe<sub>3</sub>-catalyzed aza-MBH reaction. The analysis on the basis of the absolute activation barriers indicates that the proton transfer is likely to be the rate-determining step. This

(54) In an earlier report on the NMe<sub>3</sub>-catalyzed MBH reaction between acrolein and formaldehyde, we have shown that in the presence of polar protic cocatalyst the energies of the transition states for the C–C bond formation and the proton transfer can indeed become quite comparable. See ref 18 for more details.

(55) See Table S15 in the Supporting Information for the computed relative energies for the MeOH-assisted MBH reaction.

situation arises due to the higher level of stabilization of the polar intermediates under polar solvent systems.<sup>56</sup>

## Conclusions

The mechanism of the aza-MBH reaction between acrolein and mesyl imine catalyzed by trimethylamine and trimethylphosphine has been studied by identifying all the key intermediates and transition states along the reaction pathway. The relative energies of the crucial transition states for the PMe<sub>3</sub>-catalyzed reaction have been found to be lower than those of the corresponding NMe<sub>3</sub>-catalyzed reaction, indicating a kinetic advantage for phosphine catalysts. The effect of polar protic cocatalysts/additives has been examined through the explicit consideration of cocatalysts in the transition states. The addition of the zwitterionic intermediate, originally generated by the Michael addition of the Lewis base to acrolein, to the electrophile and the intramolecular proton transfer is likely to be the rate-limiting steps depending on the reaction conditions. The energies of both C–C bond formation and proton transfer transition states in the aza-MBH reaction have been found to be lower than that known for the MBH reaction with unactivated electrophiles. The differential stabilization of the key transition states by protic cocatalyst/additive is identified as primarily arising due to the improved stabilization of the proton transfer transition state through a relay mechanism. The predicted transition state stabilization has been found to be in line with the experimentally observed rate acceleration of the (aza)-MBH reaction in the presence of polar protic cosolvent/additive. Among the three cocatalysts examined herein, formic acid has been identified as the most effective and could possibly offer improved reaction rates in the aza-MBH reaction. The results evidently point to the importance of considering explicit solvents along with continuum treatment of solvation effects in situations where high sensitivity to the nature of solvent/additives is noticed.

**Acknowledgment.** Generous computing time from the IIT Bombay computer center is acknowledged. R.B.S. acknowledges research grant-07YIA001 from Industrial Research and Consultancy Center (IRCC)-IIT Bombay through the young investigator award scheme.

**Supporting Information Available:** The optimized Cartesian coordinates, energy and geometry of various intermediates/transition states, complete citation for ref 21, and other pertinent details. This material is available free of charge via the Internet at <http://pubs.acs.org>.

(56) See Table S6 in the Supporting Information for details on the activation barriers computed with respect to the prereacting complexes or the corresponding intermediates.